

**Bias in calculating gross nitrification rates in forested catchments using the
triple oxygen isotopic composition ($\Delta^{17}\text{O}$) of stream nitrate**

Weitian Ding¹, Urumu Tsunogai¹, Fumiko Nakagawa¹

¹Graduate School of Environmental Studies, Nagoya University, Furo-cho, Chikusa-
ku, Nagoya 464-8601, Japan

Corresponding to: Weitian Ding (dwt530754556@gmail.com)

1 **Abstract**

2 A novel method has been proposed and applied in recent studies to quantify gross
3 nitrification rate (GNR) in forested catchments using the triple oxygen isotopic
4 composition ($\Delta^{17}\text{O}$) of stream nitrate. However, the equations used in these
5 calculations assume that the $\Delta^{17}\text{O}$ value of nitrate consumed through assimilation or
6 denitrification in forest soils is equal to the $\Delta^{17}\text{O}$ value of stream nitrate. The GNR
7 estimated from the $\Delta^{17}\text{O}$ value of stream nitrate was significantly higher than the
8 GNRs in our simulated calculations for a forested catchment where the soil nitrate had
9 $\Delta^{17}\text{O}$ values higher than those the stream nitrate. Because most of the reported soil
10 nitrate in forested catchments showed $\Delta^{17}\text{O}$ values higher than those of the stream
11 nitrate, we concluded that the GNR estimated from the $\Delta^{17}\text{O}$ value of stream nitrate
12 was, to an extent, an overestimate of the actual GNR.

13

14 **1 Introduction**

15 Nitrate (NO_3^-) is an important nitrogen nutrient for primary production in soils.
16 Nitrification is the microbial process that produces NO_3^- in forested ecosystems.
17 Thus, quantifying the nitrification rate can assist in the evaluation of the present and
18 future states of forested ecosystems. The net nitrification rate can be estimated from
19 an increase in NO_3^- concentration during a certain period. However, the gross
20 nitrification rate (GNR), which includes the net nitrification rate plus the consumption
21 rate of NO_3^- (e.g., through plant assimilation or denitrification), reflects the internal N
22 cycling better than the net nitrification rate (Bengtsson et al., 2003), especially in

23 forested ecosystems. Although the net nitrification rate is often negligible (Stark and
24 Hart, 1997), the consumption rate is significant in forested ecosystems, such that the
25 GNR often exceeds the net nitrification rate by several orders of magnitude (Verchot
26 et al., 2001).

27 Recent studies have successfully estimated the GNR in aquatic environments, such
28 as lakes, using the $\Delta^{17}\text{O}$ values of NO_3^- as a conservative tracer to determine the
29 mixing ratio between atmospheric nitrate ($\text{NO}_3^-_{\text{atm}}$) and biologically produced nitrate
30 ($\text{NO}_3^-_{\text{bio}}$) (Tsunogai et al., 2011, 2018). The $\text{NO}_3^-_{\text{atm}}$ is deposited in the water
31 environment, while $\text{NO}_3^-_{\text{bio}}$ is produced through nitrification. The $\text{NO}_3^-_{\text{bio}}$ always
32 shows the $\Delta^{17}\text{O}$ value close to 0 ‰ because its oxygen atoms are derived from either
33 terrestrial O_2 or H_2O through nitrification. Contrarily, the $\text{NO}_3^-_{\text{atm}}$ always displays an
34 anomalous enrichment in ^{17}O with $\Delta^{17}\text{O}$ value being approximately $+26 \pm 3$ ‰ in
35 Japan (Tsunogai et al., 2010, 2016; Ding et al., 2022, 2023) because of oxygen
36 transfers from atmospheric ozone (Michalski et al., 2003; Nelson et al., 2018).
37 Additionally, $\Delta^{17}\text{O}$ is almost stable during “mass-dependent” isotope fractionation
38 processes (Michalski et al., 2004; Tsunogai et al., 2016). This is because possible
39 variations in the $\delta^{17}\text{O}$ and $\delta^{18}\text{O}$ values during the processes of biogeochemical isotope
40 fractionation follow the relation of $\delta^{17}\text{O} \approx 0.5 \delta^{18}\text{O}$, which cancels out the variations
41 in the $\Delta^{17}\text{O}$ value. Thus, regardless of the partial consumption through denitrification
42 or assimilation after deposition in a water column, the $\Delta^{17}\text{O}$ can be used as a

43 conservative tracer of $\text{NO}_3^-_{\text{atm}}$ to calculate the mixing ratio of $\text{NO}_3^-_{\text{atm}}$ to total NO_3^-
44 ($\text{NO}_3^-_{\text{atm}}/\text{NO}_3^-_{\text{total}}$) in a water column using the following equation:
45
$$[\text{NO}_3^-_{\text{atm}}]/[\text{NO}_3^-_{\text{total}}] = [\text{NO}_3^-_{\text{atm}}]/([\text{NO}_3^-_{\text{bio}}] + [\text{NO}_3^-_{\text{atm}}]) = \Delta^{17}\text{O}/\Delta^{17}\text{O}_{\text{atm}} \quad (1)$$

46 where the $\Delta^{17}\text{O}_{\text{atm}}$ and $\Delta^{17}\text{O}$ denote the $\Delta^{17}\text{O}$ values of $\text{NO}_3^-_{\text{atm}}$ and NO_3^- dissolved in
47 the water environment, respectively. Using the $\text{NO}_3^-_{\text{atm}}/\text{NO}_3^-_{\text{total}}$ ratio estimated from
48 the $\Delta^{17}\text{O}$ value of NO_3^- in a lake water column and the deposition rate of $\text{NO}_3^-_{\text{atm}}$ into
49 the lake, the GNR (i.e., production rate of $\text{NO}_3^-_{\text{bio}}$) can be successfully estimated. This
50 approach works because the $\text{NO}_3^-_{\text{atm}}/\text{NO}_3^-_{\text{total}}$ ratios are homogeneous in the water
51 column due to the active vertical mixing; thus, we can constrain the $\text{NO}_3^-_{\text{atm}}/\text{NO}_3^-_{\text{total}}$
52 ratios of NO_3^- consumed in the lake water column (Tsunogai et al., 2011, 2018).

53 In addition to applications in water environments, the $\Delta^{17}\text{O}$ method has been
54 applied to forested catchments to determine GNR (Fang et al., 2015; Hattori et al.,
55 2019; Huang et al., 2020). Using the deposition flux of $\text{NO}_3^-_{\text{atm}}$ into the catchment
56 and the leaching flux of unprocessed $\text{NO}_3^-_{\text{atm}}$ and $\text{NO}_3^-_{\text{bio}}$ via streams, the GNR in a
57 forested catchment was estimated similarly to the estimation for water environments
58 (Fang et al., 2015). However, unlike in water environments, where the
59 $\text{NO}_3^-_{\text{atm}}/\text{NO}_3^-_{\text{total}}$ ratio of nitrate consumed in the water column can be easily
60 measured, it is often difficult to determine the $\text{NO}_3^-_{\text{atm}}/\text{NO}_3^-_{\text{total}}$ ratio of NO_3^-
61 consumed in soil layers. Consequently, past studies have approximated these values as
62 equal to those of stream NO_3^- leached from forested catchments without actual
63 observation (Fang et al., 2015, Hattori et al., 2019, Huang et al., 2020). Such an

64 approximation should be used with extreme caution, as the $\text{NO}_3^-_{\text{atm}}/\text{NO}_3^-_{\text{total}}$ ratio
65 ($\Delta^{17}\text{O}$ values) of soil NO_3^- are not always equal to those of stream NO_3^- (Hattori et
66 al., 2019, Rose, 2014, Nakagawa et al., 2018). To clarify the details of the
67 approximation and its impact on the final estimated GNR, we present an accurate
68 relationship between the $\Delta^{17}\text{O}$ of soil NO_3^- and the GNR, using basic isotope mass
69 balance equations. Thereafter, we present possible range of variation in the GNRs
70 estimated for a forested catchment, using parameters such as $\Delta^{17}\text{O}$ values of stream
71 NO_3^- reported in a past study. Finally, we compared the GNRs estimated in this study
72 with those obtained from the $\Delta^{17}\text{O}$ values of stream NO_3^- .

73

74 **2 Calculation**

75 The total mass balance equation of NO_3^- including the GNR in catchments can be
76 expressed as follows:

$$77 \text{NO}_3^-_{\text{deposition}} + \text{GNR} = \text{NO}_3^-_{\text{leaching}} + \text{NO}_3^-_{\text{uptake}} + \text{GDR} \quad (2)$$

78 where $\text{NO}_3^-_{\text{deposition}}$, GNR, $\text{NO}_3^-_{\text{leaching}}$, $\text{NO}_3^-_{\text{uptake}}$, and GDR denote the deposition flux
79 of NO_3^- into the catchment, GNR in the catchment, leaching flux of NO_3^- from the
80 catchment, uptake rate of NO_3^- in the catchment, and gross denitrification rate in the
81 catchment, respectively.

82 The isotope mass balance for each $\Delta^{17}\text{O}$ value of NO_3^- in the catchment can be
83 expressed using a similar equation:

84 $\text{NO}_3^- \text{deposition} \times \Delta^{17}\text{O}(\text{NO}_3^-)_{\text{atm}} + \text{GNR} \times \Delta^{17}\text{O}(\text{NO}_3^-)_{\text{nitrification}} = \text{NO}_3^- \text{leaching} \times \Delta^{17}\text{O}(\text{NO}$
85 $3^-)_{\text{stream}} + \text{NO}_3^- \text{uptake} \times \Delta^{17}\text{O}(\text{NO}_3^-)_{\text{uptake}} + \text{GDR} \times \Delta^{17}\text{O}(\text{NO}_3^-)_{\text{denitrification}} \quad (3)$

86 where $\Delta^{17}\text{O}(\text{NO}_3^-)_{\text{atm}}$, $\Delta^{17}\text{O}(\text{NO}_3^-)_{\text{nitrification}}$, $\Delta^{17}\text{O}(\text{NO}_3^-)_{\text{stream}}$, $\Delta^{17}\text{O}(\text{NO}_3^-)_{\text{uptake}}$, and
87 $\Delta^{17}\text{O}(\text{NO}_3^-)_{\text{denitrification}}$ denote the $\Delta^{17}\text{O}$ value of NO_3^- deposited into the catchment,
88 that of the NO_3^- bio produced through nitrification, that of the NO_3^- leached from the
89 catchment, that of the NO_3^- assimilated by plants and other organisms in the
90 catchment, and that of the NO_3^- decomposed through denitrification in the catchment,
91 respectively.

92 If the $\Delta^{17}\text{O}$ values of the NO_3^- in the forested soil layers, where the NO_3^- was
93 consumed through assimilation or denitrification, are equal to the $\Delta^{17}\text{O}$ value of NO_3^-
94 in the stream, we could obtain Eq. 4:

95 $\Delta^{17}\text{O}(\text{NO}_3^-)_{\text{uptake}} = \Delta^{17}\text{O}(\text{NO}_3^-)_{\text{denitrification}} = \Delta^{17}\text{O}(\text{NO}_3^-)_{\text{stream}} \quad (4)$

96 Consequently, by combining Eqs. 3 and 4, we could obtain Eq. 5:

97 $\text{NO}_3^- \text{deposition} \times \Delta^{17}\text{O}(\text{NO}_3^-)_{\text{atm}} + \text{GNR} \times \Delta^{17}\text{O}(\text{NO}_3^-)_{\text{nitrification}} = (\text{NO}_3^- \text{leaching} + \text{NO}_3^- \text{uptak}$
98 $e + \text{GDR}) \times \Delta^{17}\text{O}(\text{NO}_3^-)_{\text{stream}} \quad (5)$

99 We could estimate the GNR using Eq. 6 obtained from Eqs. 2 and 5 because we can
100 approximate the $\Delta^{17}\text{O}$ values of NO_3^- bio produced through nitrification

101 ($\Delta^{17}\text{O}(\text{NO}_3^-)_{\text{nitrification}}$) to 0 (Michalski et al., 2003; Tsunogai et al., 2010):

102 $\text{GNR} = \text{NO}_3^- \text{deposition} \times (\Delta^{17}\text{O}(\text{NO}_3^-)_{\text{atm}} - \Delta^{17}\text{O}(\text{NO}_3^-)_{\text{stream}}) / \Delta^{17}\text{O}(\text{NO}_3^-)_{\text{stream}} \quad (6)$

103 Eq. 6 corresponds to the equations used in previous studies to quantify the GNR in
104 the forested catchments (Eq. 4 in Fang et al., 2015; Eq. 8 in Hattori et al., 2019; Eq. 4
105 in Huang et al., 2020).

106 **3 Results and Discussion**

107 The $\Delta^{17}\text{O}$ values of NO_3^- in forested soil layers should be equal to those of stream
108 NO_3^- in Eq. 6, as presented in Eq. 4 to obtain Eq. 6. While the number of
109 simultaneous observations of the oxygen isotopes of NO_3^- in soil and stream in a
110 given forested catchment is limited (Hattori et al., 2019, Osaka et al., 2010, Rose,
111 2014, Nakagawa et al., 2018), the observations showed that the oxygen isotopic ratios
112 of soil NO_3^- are often heterogeneous. In addition, the oxygen isotopic ratios of soil
113 NO_3^- mostly exceeded those of stream NO_3^- . Different from water environments,
114 vertical mixing of water/soil is limited in forested soil, so the $\Delta^{17}\text{O}$ values of soil
115 NO_3^- are often heterogeneous. For example, Hattori et al. (2019) found a decreasing
116 $\Delta^{17}\text{O}$ trend in soil NO_3^- with depth, ranging from over +20 ‰ at the surface to less
117 than +3 ‰ at depths of 25–90 cm. Additionally, more than 60 % of the soil samples
118 exhibited $\Delta^{17}\text{O}$ values significantly higher than those of stream NO_3^- determined
119 simultaneously ($\Delta^{17}\text{O}(\text{NO}_3^-)_{\text{stream}} = +1$ to +3 ‰). A similar trend in the vertical
120 distribution was observed in the $\delta^{18}\text{O}$ values of NO_3^- in another forested catchment,
121 from above +35 ‰ at the surface soil to less than +10 ‰ at depths of 30–50 cm from
122 the soil surface (Osaka et al., 2010). In addition, most of the soil NO_3^- also exhibited
123 $\delta^{18}\text{O}$ values higher than those of the stream NO_3^- (Osaka et al., 2010). Rose (2014)

124 monitored the horizontal distribution of the $\Delta^{17}\text{O}$ of soil NO_3^- by randomly setting 15
125 tension-free lysimeters at depths of 0–10 cm in a 39-ha forested catchment. They
126 reported significantly higher $\Delta^{17}\text{O}$ values in soil NO_3^- ($+9.1 \pm 5.8$ ‰ on average) than
127 those of stream NO_3^- ($+0.5$ ‰ on average) leached from the forested catchment. As
128 most fine roots and root biomass are concentrated in the top 10 cm of the soil in
129 forested catchments (Jackson et al., 1996; Li et al., 2020), most assimilation (uptake
130 reactions) of NO_3^- should occur in that top 10 cm of soil. Consequently, the
131 significant difference in the $\Delta^{17}\text{O}$ values between soil NO_3^- and stream NO_3^- ,
132 particularly in surface soil layers, implies that the estimated GNRs in forested
133 catchments obtained from Eq. 6 were inaccurate.

134 To demonstrate the impact of this approximation on GNR estimation, we simulated
135 GNR for two different forest soils within the same catchment. In the first scenario,
136 soil NO_3^- exhibited a $\Delta^{17}\text{O}$ value close to that of $\Delta^{17}\text{O}(\text{NO}_3^-)_{\text{atm}}$ at the surface, which
137 decreased to the $\Delta^{17}\text{O}$ of stream NO_3^- at depth (heterogeneous soil) (Figs. 1a and 1b).
138 In the second scenario, soil NO_3^- had $\Delta^{17}\text{O}$ values equal to those of stream NO_3^-
139 throughout the soil profile (homogeneous soil) (Figs. 2a and 2b).

140 To simulate the forested catchment studied by Hattori et al. (2019), we used the
141 same parameters values for the current calculation, including $7.0 \text{ kg N ha}^{-1} \text{ y}^{-1}$ for
142 NO_3^- deposition, $2.6 \text{ kg N ha}^{-1} \text{ y}^{-1}$ for NO_3^- leaching, $+28.0$ ‰ for $\Delta^{17}\text{O}(\text{NO}_3^-)_{\text{atm}}$, and $+2.2$
143 ‰ for $\Delta^{17}\text{O}(\text{NO}_3^-)_{\text{stream}}$. All symbols (e.g., GNR) are consistent with those used by
144 Hattori et al. (2019).

145 To estimate GNR in each forest soil type, we divided the soils into 10 vertical
146 layers (i.e., 10 steps). In the heterogeneous soil, the $\Delta^{17}\text{O}$ values of NO_3^- gradually
147 decreased with depth, from +28.0‰ to +2.2‰, at a rate of -2.58‰ per step (Fig. 1b).
148 In the homogeneous soil, $\Delta^{17}\text{O}$ values of NO_3^- were constant at +2.2‰ across all
149 layers (Fig. 2b). Note that the y-axes in the models were layers, not depths (Tables S1,
150 S2, and S3). While the $\Delta^{17}\text{O}$ values of soil NO_3^- always showed decreasing trends
151 with depths irrespective to the seasons, $\Delta^{17}\text{O}$ values of soil NO_3^- showed significant
152 temporal variation at each depth (Hattori et al., 2019). This was the reason why the
153 layers were adopted for the y-axes in our models, instead of depths. As a result, the
154 specific depth of each layer varies over time. In addition, the relation between depth
155 and layer is not always linear. The temporal variation found in the vertical
156 distributions of $\Delta^{17}\text{O}$ values in the forested catchment (Hattori et al., 2019) can be
157 explained by our model as well without contradiction because the $\Delta^{17}\text{O}$ values of soil
158 NO_3^- , while showing large temporal variation at each depth, always showed
159 decreasing trend with depth throughout their observation (Hattori et al., 2019).

160 To estimate GNR in each layer, both the $\Delta^{17}\text{O}$ value and the NO_3^- leaching flux in
161 soil are required. While Hattori et al. (2019) reported soil NO_3^- concentrations for
162 each layer, indicating little vertical variation within the forested catchment, they did
163 not measure the catchment water flux. Consequently, it is difficult to constrain the
164 NO_3^- leaching flux for each layer of forest soil. Nevertheless, NO_3^- deposition was 7.0 kg
165 $\text{N ha}^{-1} \text{y}^{-1}$ and NO_3^- leaching was 2.6 kg $\text{N ha}^{-1} \text{y}^{-1}$ in the catchment (Hattori et al.,

166 2019). Additionally, because water fluxes decrease gradually with depth in various
167 forest settings (e.g., Christiansen et al., 2006), we assumed a gradual decrease in
168 NO_3^- , leaching flux from 7.0 to 2.6 $\text{kg N ha}^{-1} \text{y}^{-1}$ at a rate of $-0.44 \text{ kg N ha}^{-1} \text{y}^{-1}$ per
169 layer (Figs. 1c and 2c). Similar trends in the NO_3^- leaching flux of soil have been
170 observed in other forested catchments (Callesen et al., 1999; Inoue et al., 2021).

171 Applying the total mass balance and isotope mass balance equations (Eqs. 2 and 3)
172 to each layer, we estimated GNR (Figs. 1e and 2e) and the total consumption rate of
173 NO_3^- (GDR + uptake) (Figs. 1d and 2d) in each layer. In this calculation, we assumed
174 the following: (1) $\Delta^{17}\text{O}$ values of NO_3^- were constant in each layer; (2) vertical flow
175 of NO_3^- in soil layers proceeds downward from the surface to the final layer (No. 10);
176 and (3) GNR and the NO_3^- consumption rate (GDR + uptake) are 0 in layers beyond
177 the final layer. By summing the GNR determined for each layer, we estimated the
178 total GNR in the forested catchment.

179 The total GNR estimated for the catchment with the homogeneous $\Delta^{17}\text{O}$ values in
180 soil NO_3^- (homogeneous soil) was 83.6 $\text{kg of N ha}^{-1} \text{y}^{-1}$ (Fig. 2e), exactly equal to
181 that estimated by Hattori et al. (2019) using Eq. 6. This result allows us to further
182 verify that past studies estimating GNR using Eq. 6 implicitly approximated that $\Delta^{17}\text{O}$
183 values of soil NO_3^- consumed in forested catchments were homogeneous and always
184 equal to those of stream NO_3^- . However, the total GNR estimated for the catchment
185 with heterogeneous $\Delta^{17}\text{O}$ values in soil NO_3^- (heterogeneous soil) was considerably

186 lower ($13.0 \text{ kg of N ha}^{-1} \text{ y}^{-1}$; Fig. 1e), while the same parameters were used for
187 NO_3^- deposition, NO_3^- leaching, $\Delta^{17}\text{O}(\text{NO}_3^-)_{\text{atm}}$, and $\Delta^{17}\text{O}(\text{NO}_3^-)_{\text{stream}}$.

188 As we increased the number of layers in the forest soils to 20, 30, 50, 100, and
189 1000, the estimated GNR for the heterogeneous soil decreased to 11.4, 11.0, 10.5,
190 10.3, and $10.1 \text{ kg N ha}^{-1} \text{ y}^{-1}$, respectively. Moreover, when we changed the
191 calculation method from stepwise summation to integration, the estimated GNR was
192 $11.2 \text{ kg N ha}^{-1} \text{ y}^{-1}$. Furthermore, even if we assumed non-linear variation for the
193 leaching flux of soil NO_3^- , in which the leaching flux of soil NO_3^- increased with soil
194 depth from layers 1 to 5 with an increasing rate of $0.44 \text{ kg of N ha}^{-1} \text{ y}^{-1} \text{ layer}^{-1}$, while
195 the leaching flux decreased with soil depth from layers 6 to 10 with a decreasing rate
196 of $1.32 \text{ kg of N ha}^{-1} \text{ y}^{-1} \text{ layer}^{-1}$ (Table S3), the newly estimated total GNR (19.1 kg of
197 $\text{N ha}^{-1} \text{ y}^{-1}$) was still comparable with that estimated for the forested catchment with
198 the heterogeneous soil shown by Figure 1 ($13.0 \text{ kg of N ha}^{-1} \text{ y}^{-1}$). As a result, we
199 concluded that the differences in the $\Delta^{17}\text{O}$ values of the soil NO_3^- consumed in a
200 forested catchment from that of stream NO_3^- resulted in a significant deviation in the
201 GNR estimated using Eq. 6 from the actual GNR. In addition, the most important
202 parameter to determine GNR was the $\Delta^{17}\text{O}$ values of NO_3^- consumed in soil layers.
203 That is, the other parameters such as the number of layers and the vertical changes in
204 the leaching flux of soil NO_3^- had little impact on total GNR.

205 By combining the total mass balance and isotope mass balance shown in Eqs. 2 and
206 3, Eq. 7 was obtained to accurately estimate the total GNR:

$$\text{GNR} = \text{NO}_3^- \text{leaching} - \text{NO}_3^- \text{deposition} + (\text{NO}_3^- \text{deposition} \times \Delta^{17}\text{O}(\text{NO}_3^-)_{\text{atm}} - \text{NO}_3^- \text{leaching} \times \Delta^{17}\text{O}(\text{NO}_3^-)_{\text{stream}}) / \Delta^{17}\text{O}(\text{NO}_3^-)_{\text{soil}} \quad (7)$$

where $\Delta^{17}\text{O}(\text{NO}_3^-)_{\text{soil}}$ denotes the “average” $\Delta^{17}\text{O}$ of NO_3^- consumed through assimilation or denitrification in the forested catchment. Most of the soil NO_3^- measured to date exhibited $\Delta^{17}\text{O}$ values higher than those of stream NO_3^- leached from the catchments (Hattori et al., 2019, Rose, 2014). Consequently, the total GNR estimated from stream NO_3^- using Eq. 6 exceeded the total GNR estimated from soil NO_3^- using Eq. 7, to an extent. Therefore, the total GNR estimated from Eq. 6 was overestimated to an extent.

If we can estimate the downward water flux at each soil layer, along with the NO_3^- concentration and $\Delta^{17}\text{O}$ value of NO_3^- in each soil layer using, e.g., a tension-free lysimeter (Inoue et al., 2021), we could estimate the vertical change in the NO_3^- leaching flux for each soil layer, along with the $\Delta^{17}\text{O}$ values of soil NO_3^- . Thereafter, applying Eq. 7 to each layer, we can more estimate the total GNR for the forested catchment accurately, by integrating the GNR estimated for each soil layer, together with the NO_3^- consumption rate in the forested catchment.

223

224 **4 Conclusion**

225 Past studies have proposed the $\Delta^{17}\text{O}$ method for determining the GNR in forested
 226 catchments. The equations used in the calculation implicitly assumed that the $\Delta^{17}\text{O}$
 227 values of NO_3^- consumed in forested soils are homogeneous and equal to those of the

228 stream NO_3^- . However, the values are often heterogeneous and do not always equal
229 those of the stream in forested soils. It is essential to clarify/verify the $\Delta^{17}\text{O}$ values of
230 NO_3^- in forested soils and streams before applying the $\Delta^{17}\text{O}$ values of stream NO_3^- to
231 estimate the total GNR.

232

233 *Data availability.* All data are presented in the Supplement.

234

235 *Author contributions.* WD, UT, and FN designed the study. WD and UT performed
236 data analysis and wrote the paper.

237

238 *Competing interests.* The authors declare that they have no conflict of interest.

239

240 *Acknowledgments*

241 We thank Dr. Joel Bostic, Dr. Lucy Rose and other two anonymous referees for
242 their valuable remarks on an earlier version of this paper. We are grateful to the
243 members of the Biogeochemistry Group, Nagoya University, for their valuable
244 support throughout this study. This work was supported by a Grant-in-Aid for
245 Scientific Research from the Ministry of Education, Culture, Sports, Science, and
246 Technology of Japan under grant numbers 22H00561, 17H00780, 22K19846, the
247 Grant-in-Aid for JSPS Fellows under grant number 23KJ1088, the Yanmar
248 Environmental Sustainability Support Association, and the river fund of the river

249 foundation, Japan. Weitian Ding would like to take this opportunity to thank the
250 “Nagoya University Interdisciplinary Frontier Fellowship” supported by Nagoya
251 University and JST, the establishment of university fellowships towards the creation
252 of science technology innovation, Grant Number JPMJFS2120.

253

254 **References**

255 Bengtsson, G., Bengtson, P. and Månsson, K. F.: Gross nitrogen mineralization-,
256 immobilization-, and nitrification rates as a function of soil C/N ratio and microbial
257 activity, *Soil Biol. Biochem.*, 35(1), 143–154, doi:10.1016/S0038-0717(02)00248-1,
258 2003.

259 Callesen, I., Raulund-Rasmussen, K., Gundersen, P., and Stryhn, H.: Nitrate
260 concentrations in soil solutions below Danish forests, *Forest Ecology and*
261 *Management*, 114, 71–82, [https://doi.org/10.1016/S0378-1127\(98\)00382-X](https://doi.org/10.1016/S0378-1127(98)00382-X), 1999.

262 Christiansen, J. R., Elberling, B., and Jansson, P.-E.: Modelling water balance and
263 nitrate leaching in temperate Norway spruce and beech forests located on the same
264 soil type with the CoupModel, *Forest Ecology and Management*, 237, 545–556,
265 <https://doi.org/10.1016/j.foreco.2006.09.090>, 2006.

266 Ding, W., Tsunogai, U., Nakagawa, F., Sambauchi, T., Sase, H., Morohashi, M., and
267 Yotsuyanagi, H.: Tracing the source of nitrate in a forested stream showing elevated
268 concentrations during storm events, *Biogeosciences*, 19, 3247–3261,
269 <https://doi.org/10.5194/bg-19-3247-2022>, 2022.

270 Ding, W., Tsunogai, U., Nakagawa, F., Sambuichi, T., Chiwa, M., Kasahara, T., and
271 Shinozuka, K.: Stable isotopic evidence for the excess leaching of unprocessed
272 atmospheric nitrate from forested catchments under high nitrogen saturation,
273 *Biogeosciences*, 20, 753–766, <https://doi.org/10.5194/bg-20-753-2023>, 2023.

274 Fang, Y., Koba, K., Makabe, A., Takahashi, C., Zhu, W., Hayashi, T., Hokari, A. A.,
275 Urakawa, R., Bai, E., Houlton, B. Z., Xi, D., Zhang, S., Matsushita, K., Tu, Y., Liu,
276 D., Zhu, F., Wang, Z., Zhou, G., Chen, D., Makita, T., Toda, H., Liu, X., Chen, Q.,
277 Zhang, D., Li, Y. and Yoh, M.: Microbial denitrification dominates nitrate losses from
278 forest ecosystems, *Proc. Natl. Acad. Sci. U. S. A.*, 112(5), 1470–1474,
279 [doi:10.1073/pnas.1416776112](https://doi.org/10.1073/pnas.1416776112), 2015.

280 Hattori, S., Nuñez Palma, Y., Itoh, Y., Kawasaki, M., Fujihara, Y., Takase, K. and
281 Yoshida, N.: Isotopic evidence for seasonality of microbial internal nitrogen cycles in
282 a temperate forested catchment with heavy snowfall, *Sci. Total Environ.*, 690, 290–
283 299, [doi:10.1016/j.scitotenv.2019.06.507](https://doi.org/10.1016/j.scitotenv.2019.06.507), 2019.

284 Huang, S., Wang, F., Elliott, E. M., Zhu, F., Zhu, W., Koba, K., Yu, Z., Hobbie, E.
285 A., Michalski, G., Kang, R., Wang, A., Zhu, J., Fu, S. and Fang, Y.: Multiyear
286 Measurements on $\Delta^{17}\text{O}$ of Stream Nitrate Indicate High Nitrate Production in a
287 Temperate Forest, *Environ. Sci. Technol.*, 54(7), 4231–4239,
288 [doi:10.1021/acs.est.9b07839](https://doi.org/10.1021/acs.est.9b07839), 2020.

289 Inoue, T., Nakagawa, F., Shibata, H. and Tsunogai, U.: Vertical Changes in the Flux
290 of Atmospheric Nitrate From a Forest Canopy to the Surface Soil Based on $\Delta^{17}\text{O}$

291 Values, *J. Geophys. Res. Biogeosciences*, 126(4), 1–18, doi:10.1029/2020JG005876,
292 2021.

293 Jackson, R. B., Canadell, J., Ehleringer, J. R., Mooney, H. A., Sala, O. E. and
294 Schulze, E. D.: A global analysis of root distributions for terrestrial biomes,
295 *Oecologia*, 108(3), 389–411, doi:10.1007/BF00333714, 1996.

296 Li, F. L., McCormack, M. L., Liu, X., Hu, H., Feng, D. F., and Bao, W. K.: Vertical
297 fine-root distributions in five subalpine forest types shifts with soil properties across
298 environmental gradients, *Plant Soil*, 456, 129–143, [https://doi.org/10.1007/s11104-](https://doi.org/10.1007/s11104-020-04706-x)
299 [020-04706-x](https://doi.org/10.1007/s11104-020-04706-x), 2020.

300 Michalski, G., Scott, Z., Kabling, M. and Thiemens, M. H.: First measurements and
301 modeling of $\Delta^{17}\text{O}$ in atmospheric nitrate, *Geophys. Res. Lett.*, 30(16), 3–6,
302 doi:10.1029/2003GL017015, 2003.

303 Michalski, G., Meixner, T., Fenn, M., Hernandez, L., Sirulnik, A., Allen, E. and
304 Thiemens, M.: Tracing Atmospheric Nitrate Deposition in a Complex Semiarid
305 Ecosystem Using $\Delta^{17}\text{O}$, *Environ. Sci. Technol.*, 38(7), 2175–2181,
306 doi:10.1021/es034980+, 2004.

307 Nakagawa, F., Tsunogai, U., Obata, Y., Ando, K., Yamashita, N., Saito, T.,
308 Uchiyama, S., Morohashi, M. and Sase, H.: Export flux of unprocessed atmospheric
309 nitrate from temperate forested catchments: A possible new index for nitrogen
310 saturation, *Biogeosciences*, 15(22), 7025–7042, doi:10.5194/bg-15-7025-2018, 2018.

311 Nelson, D. M., Tsunogai, U., Ding, D., Ohyama, T., Komatsu, D. D., Nakagawa, F.,
312 Noguchi, I. and Yamaguchi, T.: Triple oxygen isotopes indicate urbanization affects
313 sources of nitrate in wet and dry atmospheric deposition, *Atmos. Chem. Phys.*, 18(9),
314 6381–6392, doi:10.5194/acp-18-6381-2018, 2018.

315 Osaka, K., Ohte, N., Koba, K., Yoshimizu, C., Katsuyama, M., Tani, M., Tayasu, I.
316 and Nagata, T.: Hydrological influences on spatiotemporal variations of $\delta^{15}\text{N}$ and
317 $\delta^{18}\text{O}$ of nitrate in a forested headwater catchment in central Japan: Denitrification
318 plays a critical role in groundwater, *J. Geophys. Res. Biogeosciences*, 115(G2), n/a-
319 n/a, doi:10.1029/2009jg000977, 2010.

320 Rose, L. A.: Assessing the nitrogen saturation status of appalachian forests using
321 stable isotopes of nitrate [PhD thesis, University of Pittsburgh]. Retrieved from
322 http://d-scholarship.pitt.edu/22783/1/LRose_ETD_081914_revised1.pdf.

323 Stark, J. M. and Hart, S. C.: High rates of nitrification and nitrate turnover in
324 undisturbed coniferous forests, *Nature*, 385(6611), 61–64, doi:10.1038/385061a0,
325 1997.

326 Tsunogai, U., Komatsu, D. D., Daita, S., Kazemi, G. A., Nakagawa, F., Noguchi, I.
327 and Zhang, J.: Tracing the fate of atmospheric nitrate deposited onto a forest
328 ecosystem in Eastern Asia using $\Delta^{17}\text{O}$, *Atmos. Chem. Phys.*, 10(4), 1809–1820,
329 doi:10.5194/acp-10-1809-2010, 2010.

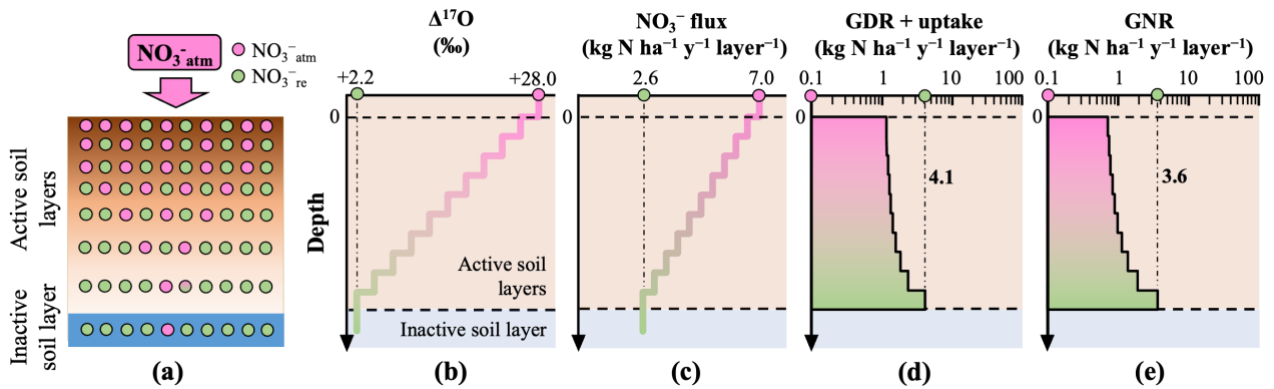
330 Tsunogai, U., Daita, S., Komatsu, D. D., Nakagawa, F. and Tanaka, A.: Quantifying
331 nitrate dynamics in an oligotrophic lake using $\Delta^{17}\text{O}$, *Biogeosciences*, 8(3), 687–702,
332 doi:10.5194/bg-8-687-2011, 2011.

333 Tsunogai, U., Miyauchi, T., Ohyama, T., Komatsu, D. D., Nakagawa, F., Obata, Y.,
334 Sato, K. and Ohizumi, T.: Accurate and precise quantification of atmospheric nitrate
335 in streams draining land of various uses by using triple oxygen isotopes as tracers,
336 *Biogeosciences*, 13(11), 3441–3459, doi:10.5194/bg-13-3441-2016, 2016.

337 Tsunogai, U., Miyauchi, T., Ohyama, T., Komatsu, D. D., Ito, M. and Nakagawa, F.:
338 Quantifying nitrate dynamics in a mesotrophic lake using triple oxygen isotopes as
339 tracers, *Limnol. Oceanogr.*, 63, S458–S476, doi:10.1002/lno.10775, 2018.

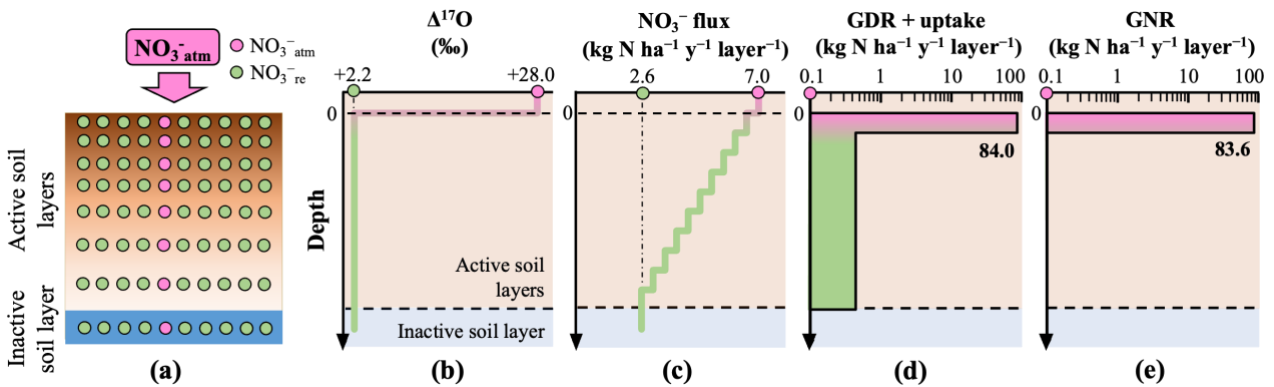
340 Verchot, L. V., Holmes, Z., Mulon, L., Groffman, P. M. and Lovett, G. M.: Gross vs
341 net rates of N mineralization and nitrification as indicators of functional differences
342 between forest types, *Soil Biol. Biochem.*, 33(14), 1889–1901, doi:10.1016/S0038-
343 0717(01)00095-5, 2001.

344



345 **Figure. 1.** Distribution of $\text{NO}_3^-_{\text{atm}}$ in the simulated forested soil with heterogeneous
 346 distribution of $\Delta^{17}\text{O}$ values of NO_3^- (a). Vertical distribution of the following
 347 parameters in the forested soil: assumed $\Delta^{17}\text{O}$ values of NO_3^- (b), assumed leaching
 348 flux of NO_3^- (c), estimated NO_3^- consumption rate (GDR + uptake) (d), and estimated
 349 GNR (e).

350



351 **Figure. 2.** Distribution of $\text{NO}_3^-_{\text{atm}}$ in the simulated forested soil with homogeneous
 352 distribution of $\Delta^{17}\text{O}$ values of NO_3^- (a). Vertical distribution of the following
 353 parameters in the forested soil: assumed $\Delta^{17}\text{O}$ values of NO_3^- (b), assumed leaching
 354 flux of NO_3^- (c), estimated NO_3^- consumption rate (GDR + uptake) (d), and estimated
 355 GNR (e).